# Recent results for single meson production from the Crystal-Barrel/TAPS experiment at ELSA *

R. Beck[1)] (for the CBELSA/TAPS collaboration)

(HISKP University of Bonn, 53115 Bonn, Germany)

**Abstract** The present focus of the CBELSA/TAPS experiment is on meson-photoproduction off the nucleon using polarized photons and polarized targets. Here first preliminary results on the reactions $\vec{\gamma}\vec{\mathrm{p}} \to \mathrm{p}\pi^0$ and $\vec{\gamma}\vec{\mathrm{p}} \to \mathrm{p}\eta$ for both circularly and linearly polarized photons and a longitudinally polarized target are presented. Preliminary results for the beam asymmetry $\Sigma$ and the double polarization observable $G$ have been extracted for both reactions using the linear polarization data. From the circular polarization data the observable $E$ has been determined. Due to the near $4\pi$ angular coverage of the detector system these results cover almost the full solid angle.

**Key words** meson photoproduction, double polarization, baryon spectroscopy

**PACS** 13.60.-r, 13.60.Le, 13.88.+e

## 1 Introduction

The determination of the dynamics underlying meson-photoproduction has, for several decades, been a major challenge in hadronic physics. However, despite this long history and a large experimental effort, the reaction mechanisms are still far from being understood, mainly due to contributions from a substantial number of hadronic resonances which are difficult to disentangle. New perspectives for the study of these resonances have been opened by the possibility of performing experiments using polarized photons and polarized targets.

The central goal of the experimental program within the CBELSA/TAPS collaboration is to perform precise measurements on photoproduction of mesons off the nucleon in the mass region up to 2.5 GeV with explicit inclusion of polarization degrees of freedom to extract information on the dynamics of the production process and on the baryon spectrum. Of crucial importance for a detailed understanding of the baryon spectrum is the measurement of single and double polarization observables to reduce the existing ambiguities in the partial wave analysis and to increase the sensitivity on small resonance contributions. The final goal is of course to get as close as possible to a complete data base, which would allow for a model independent partial wave analysis.

## 2 Polarization observables

For a complete data base, allowing for a model independent partial wave analysis, eight carefully chosen observables need to be measured [1].

Table 1 shows the observables accessible for single pseudoscalar meson-photoproduction, some of which have been already measured ($\sigma$, $\Sigma$) at ELSA for $\mathrm{p}\pi^0$ [2] and $\mathrm{p}\eta$ [3]. $G$ and $E$ are presently measured with a longitudinally polarized target and linearly and circularly polarized photons. The observables $H$, $P$ and $F$ will become accessible using a transversally polarized target.

A complete data base for pseudoscalar meson photoproduction (the "complete" experiment) requires at least eight independent observables to be measured. Such complete information is not available at present, however, close to thresholds or in the $P_{33}(1232)$ resonance region where only a few partial waves contribute, an almost model-independent analysis can be performed. This has been demonstrated in the

Received 7 August 2009

* Supported within the SFB/TR16 by the Deutsche Forschungsgemeinschaft (DFG)

1) E-mail: beck@hiskp.uni-bonn.de

$s$- and $p$-wave determination at the $\pi^0$-threshold [4], where information on the differential cross section $\frac{d\sigma}{d\Omega}$ and the photon beam asymmetry ($\Sigma$) were sufficient to determine the four $s$- and $p$-wave amplitudes ($E_{0+}, M_{1+}, M_{1-}$ and $E_{1+}$). Another nice example is the determination of the E2/M1- ratio of the $P_{33}(1232)$-resonance. Again precise data on $\frac{d\sigma}{d\Omega}$ and $\Sigma$ for the reactions $\vec{\gamma}p \to p\pi^0$ and $\vec{\gamma}p \to n\pi^+$ have been used to determine the isospin 1/2 and 3/2 contributions of the four $s$- and $p$-waves[5]. One important constraint in this analysis is the Fermi-Watson theorem[6]. The multipole amplitudes $M^I_{l\pm}$ are complex functions of the c.m. energy $W$. Below the two-pion production threshold, the Fermi-Watson theorem allows one to express the phases of the complex multipole amplitudes by the corresponding pion-nucleon scattering phase shifts $\delta^I_{l\pm}$.

$$M^I_{l\pm} = |M^I_{l\pm}| \cdot \exp(i\delta^I_{l\pm} + n\pi)$$

where $I$ is the isospin (1/2 or 3/2), $l$ is the angular momentum of the outgoing pion and n is an integer. Without the Fermi-Watson theorem one has to rely on $\frac{d\sigma}{d\Omega}$, $\Sigma$, $T$ and $P$. For pion photoproduction from threshold up to the $P_{33}(1232)$ resonance region, these four observables provide sufficient constraints for a complete data base, if the higher partial waves can be adequately represented by the Born contributions. Such arguments were used by Grushin[7] to analyse the Kharkov data. In their analysis both the real and imaginary parts for the $s$- and $p$-wave amplitudes could be determined for the first time independently of the pion-nucleon phase shifts. The mean difference between the phase shift $\delta_{33}$ from the Kharkov analysis and the known pion-nucleon scattering phase was only $(2.3 \pm 0.5)$ degrees over the entire energy range $E_\gamma = 250 - 500$ MeV. This approach is expected to appropriate up to the second resonance region.

By careful selection of the new observables, enhanced sensitivities to specific electromagnetic multipoles and, consequentially, to a few selected nucleon resonances, are obtained. For example the measurement of the helicity dependence, using circularly polarized photon beam and longitudinally polarized target, of the $\vec{\gamma}\vec{p} \to p\pi^0$ process in the second resonance region where several overlapping states are present ($P_{11}(1440) \to M_{1-}$, $D_{13}(1520) \to E_{2-}, M_{2-}$ and $S_{11}(1535) \to E_{0+}$) has been proven to be sensitive on the $E_{2-}$ and $M_{2-}$ partial waves, which strongly couple to the $D_{13}(1520)$ resonance [8]. A large sensitivity to the $M_{1-}$ partial wave amplitude and therefore the $P_{11}(1440)$ and $P_{11}(1710)$ resonances is given by the double polarization observable $G$, that can be measured using linearly polarized photons and a longitudinally polarized target.

Table 1. Observables in single pseudoscalar meson photoproduction. The observables $\sigma$ and $\Sigma$ have been measured in the past, $G$ and $E$ are presently measured using a longitudinally polarized target and a linearly or circularly polarized photon beam. The observables $H$, $P$, $T$ and $F$ are accessible with a transversally polarized target and a polarized or unpolarized beam, if the recoil polarization is not measured.

| photon | | target | | | recoil | | | target–recoil | | | |
|---|---|---|---|---|---|---|---|---|---|---|---|
| | | | | | $x'$ | $y'$ | $z'$ | $x'$ | $x'$ | $z'$ | $z'$ |
| | | $x$ | $y$ | $z$ | | | | $x$ | $z$ | $x$ | $z$ |
| unpolarized | $\sigma$ | 0 | $T$ | 0 | 0 | $P$ | 0 | $T_{x'}$ | $-L_{x'}$ | $T_{z'}$ | $L_{z'}$ |
| linear | $(-\Sigma)$ | $H$ | $(-P)$ | $(-G)$ | $O_{x'}$ | $(-T)$ | $O_{z'}$ | $(-L_{z'})$ | $(T_{z'})$ | $(-L_{x'})$ | $(-T_{x'})$ |
| circularly | 0 | $F$ | 0 | $(-E)$ | $(-C_{x'})$ | 0 | $(-C_{z'})$ | 0 | 0 | 0 | 0 |

## 3 Experimental setup

### 3.1 The photon tagging system

The CBELSA/TAPS tagging system consists of two detector components. One is composed of 96 overlapping plastic scintillator bars of varying width covering a range of 18% to 95% of the primary electron beam energy. Furthermore a two-layered hodoscope of 480 scintillating fibres provides an enhanced rate stability and resolution for the lower end of the photon energy range. With this setup an energy resolution of 0.2% to 2.2% is achieved.

### 3.2 Polarized photon beams

The CBELSA/TAPS experiment has access to both linearly and circularly polarized photons.

The linearly polarized photons are be produced by coherent bremsstrahlung off a diamond crystal radiator. The use of this method furtheron increases the photon flux in the selected region of polarization (see Fig. 1). The option to rotate the photons'

polarization vector by 90° by realigning the crystal allows to effectively determine the intrinsic detector $\varphi$-dependence.

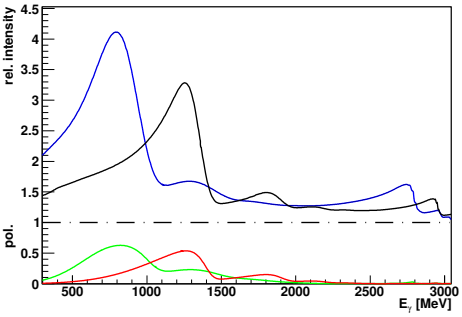


Fig. 1. Normalized bremsstrahlspectrum for the settings given above (blue: 950 MeV, black 1350 MeV). The lower curve (green: 950 MeV, red: 1350 MeV) indicates the degree of polarization.

Circularly polarized photons are produced by bremsstrahlung off an amorphous radiator. The according helicity transfer is show in Fig. 2. Scattering the polarized electron beam on a Møller target allows for simultaneous measurement of the achieved degree of (electron) polarization.

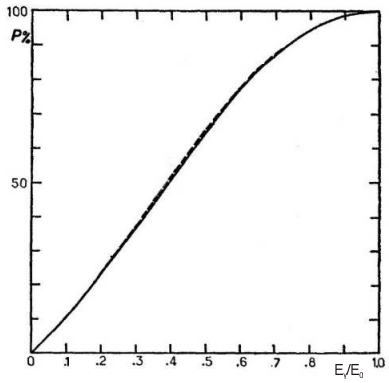


Fig. 2. Energy dependent polarization transfer in units of $E_\gamma/E_e$.

### 3.3 Target polarization

For double polarization measurements the Bonn frozen spin butanol target was used. For the recent measurements the target cryostat was equipped with a longitudinal holding coil, providing longitudinally polarized protons. For future measurements the current coil will be replaced with a saddle type superconducting holding coil (see Fig. 3) producing a transverse magnetic field. The material budget for these coils is very low, so that produced particles can pass virtually unaffected.

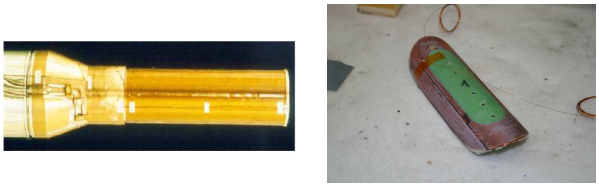

Fig. 3. The longitudinal (left) and new transverse (right) holding coils.

The target material is butanol ($C_4H_9OH$) which has an effective density of 0.57 g/cm$^3$ and a dilution factor of $D$=0.1335. In the past a typical mean polarization of around 70% has been reached. In general a maximum polarization of 90% is possible. The relaxation time of the target is in the order of 600 h. The target properties are given as a reference in Table 2.

Table 2. Parameters of the Bonn frozen spin butanol target.

| | |
|---|---|
| material | $C_4H_9OH$ |
| dilution factor | 10/74 |
| length | 18.8±0.15 mm |
| diameter | 2 cm |
| density at 1 K | 0.94 g/cm$^3$ |
| filling factor | 60.7±1.5% |
| density (eff.) | 0.57g/cm$^3$ |
| mean polarization | 70% |
| time for repolarization | 4-5 h |
| target area density | $8.62\pm0.24\cdot10^{22}$/cm$^2$ |

### 3.4 Detector configuration

The Crystal Barrel calorimeter consisting of 1230 CsI(Tl)-crystals is complemented by two additional detector systems. The forward detector and the Mini-TAPS array. These forward detectors close the forward angular range of ±30°. The forward detector consists of 90 CsI(Tl) crystals covering the angular range between 30° and 12°. The Mini-TAPS array (216 $BaF_2$-crystals) covers the angular range further down to 1.2°. While the Crystal Barrel CsI(Tl)-crystals are read out by photodiodes, the forward detector crystals utilize photomultipliers. These give the forward detector trigger capabilities and allows timing measurements. The time resolution achieved with this crystal-lightguide-photomultiplier configuration is about 4 ns (FWHM) which is sufficient for its inclusion in the first level trigger.

Plastic scintillators are placed in front of the crystals of both forward detectors to identify charged particles. For the forward detector a double layer of 180 plastic scintillators of 3 mm thickness is placed in front of the crystals. The front faces of MiniTAPS

$BaF_2$ crystals are also covered by plastic scintillator plates. Each scintillator of both of the detectors is read out by two wavelengthshifting/lightguide fibres, delivering an optimum performance regarding lightoutput and signal to noise ratio. For charged particle detection inside the Crystal Barrel calorimeter a fibre detector consisting of 513 fibres in a total of three layers (orientation: $\pm 25°, 0°$) is installed around the target cryostat. This arrangement allows the three-dimensional reconstruction of the penetration point of the charged trajectory with the inner detector. To suppress electromagnetic background from e.g. pair-production a $CO_2$-Gas-Čerenkov detector has been installed between the forward detector and MiniTAPS. Its efficiency is well above 99.9% for electrons/positrons above 25 MeV, whereas its sensitivity to pions starts at about 4 GeV which is above the maximum beam energy provided by ELSA. Further on the CBELSA/TAPS experiment features two detectors to determine the photon flux for absolute normalization of the taken data. The setup of the complete CBELSA/TAPS experiment at ELSA is given in Fig. 4.

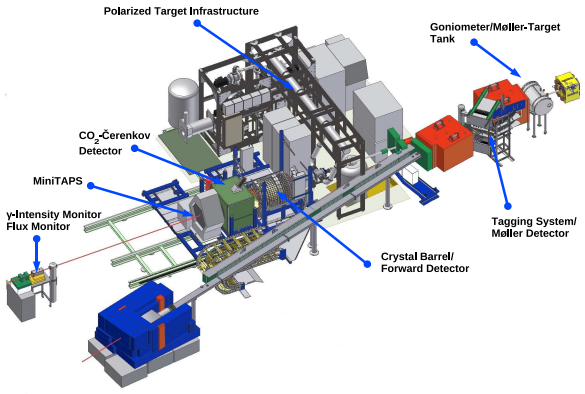


Fig. 4. Overview of the experimental setup.

## 4 Recent double polarization measurements

With the aforementioned setup the Crystal-Barrel/TAPS experiment can access the following observables in single meson photoproduction. For linearly polarized photons the polarization observables $\Sigma$ and $G$ are accessible. For circularly polarized photons $E$ can be measured. Due to the detectors' large acceptance the (unpolarized) differential cross section can be measured over the full solid angle. The differential cross section for the observables accessible using a polarized photon beam and a longitudinally polarized target with $p_\gamma$ and $p_z$ being the respective degrees of polarization can be written as follows:

$$\frac{\mathrm{d}\sigma}{\mathrm{d}\Omega}(\theta,\phi) = \frac{\mathrm{d}\sigma}{\mathrm{d}\Omega}(\theta)\cdot[1 - p_\gamma^{\mathrm{lin}}\Sigma(\theta)\cos(2\phi) - p_z\cdot(-p_\gamma^{\mathrm{lin}}G(\theta)\sin(2\phi) + p_\gamma^{\mathrm{circ}}E(\theta)].$$

The definition of the angles is illustrated in Fig. 5. The incoming photon and the outgoing proton define the reaction plane. The angle between the photon directon $z$ and the outgoing meson defines $\Theta$. For linearly polarized photons, the angle $\phi$ is defined as the angle between the polarization vector of the incoming photon and the reaction plane.

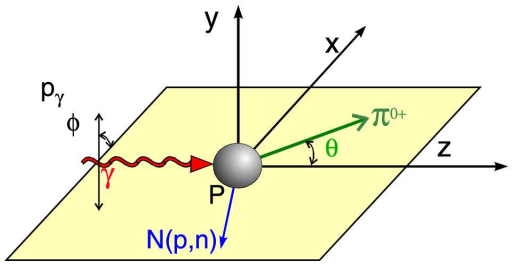


Fig. 5. Single meson production demonstrated on the reaction $\vec{\gamma}\vec{\mathrm{p}} \to \mathrm{p}\pi^0$.

First preliminary double polarization results in two meson photoproduction are presented in the contribution of $U$. Thoma[9] and for $\omega$-photoproduction by H. Schmieden[10].

1) Measurement with circularly polarized photons and a longitudinally polarized target.

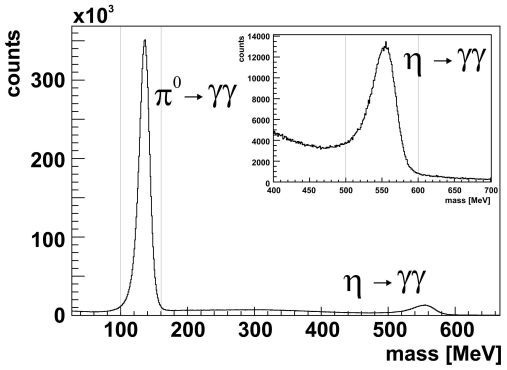


Fig. 6. Invariant $\gamma\gamma$-mass distribution for events with a charged particle and two photons in the final state after a coplanarity and a missing mass cut was performed. Analysis and calibration: preliminary (only part of the statistics shown). The vertical (red) lines indicate the $\pi^0$- and $\eta$-mass cut used.

Figures 6 and 7 give an impression of the quality of the double polarization data taken with the CBELSA/TAPS experiment at ELSA. Even though the data selection as well as the calibration is still

very preliminary Fig. 6 shows clear $\pi^0$- and $\eta$-signals above a small background, which will be reduced further by a more refined analysis.

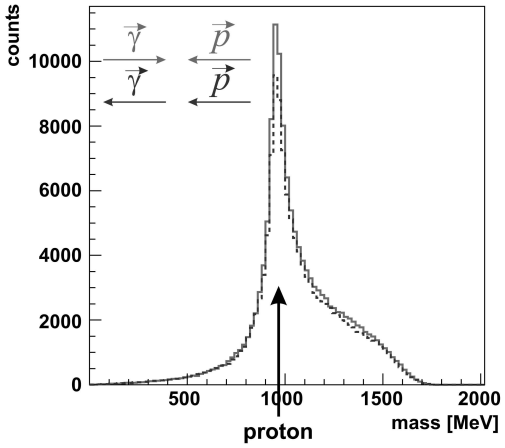


Fig. 7. Missing mass distribution for events which are consistent with $\vec{\gamma}\vec{p} \to X\eta$ after having performed a cut on the mass of the $\eta$ and a coplanarity cut. Events with helicity 1/2 are plotted as solid (red) line, events with helicity 3/2 as dashed (blue) line. A clear count rate difference is observed in the proton mass region. Preliminary analysis and calibration, only part of the statistics shown.

Plotting the missing mass distribution for events being consistent with $\vec{\gamma}\vec{p} \to X\eta$ using the $\eta$ cut indicated in Fig. 6, Fig. 7 is obtained. This figure shows the comparison of the missing mass for events where the spin of photon and proton were parallel in comparison to the ones where they are anti-parallel. For events with a missing mass being consistent with the proton a clear count rate difference $N_{1/2} - N_{3/2}$ is observed; the events with helicity 1/2 dominate over the events with helicity 3/2.

Figure 8 shows this count rate difference as a function of the incoming photon energy. As expected, $N_{1/2}$ dominates at low energies. This is due to the dominance of the $S_{11}(1535)$ close to threshold. This behaviour is also clearly visible in all different PWA-predictions for $\sigma_{1/2} - \sigma_{3/2}$. Deviations between the different PWA-solutions occur in the area above $E_\gamma$=1000 MeV. The region around $E_\gamma$=1100 MeV is of particluar interest. Here clear deviations are observed in the different PWA predictions. While the solution of the BnGa-PWA published in [11] allows, within errors, for negative values in $\sigma_{1/2} - \sigma_{3/2}$ up to slightly positive values, the MAID solution shows a clear positive value (Fig. 8). The main difference between the BnGa and MAID solution is a strong contribution of the $P_{11}(1710)$ in MAID, which is not needed in the BnGa-PWA, while in this case the $P_{13}(1720)$ contributes quite strongly. A very preliminary comparison with the data, which are not corrected for acceptance, nor has the polarization or the flux been taken into account, indicates that the helicity difference might indeed be positive. More information will be provided by the according differential distributions, which cover nearly the full angular range.

Figure 9 shows the according distributions for the $p\pi^0$ final state[12]. The energy dependent count rate difference $N_{1/2}$-$N_{3/2}$ indicates resonance structures, starting at low energies, where the $\Delta(1232)$ dominates, as expected at negative values.

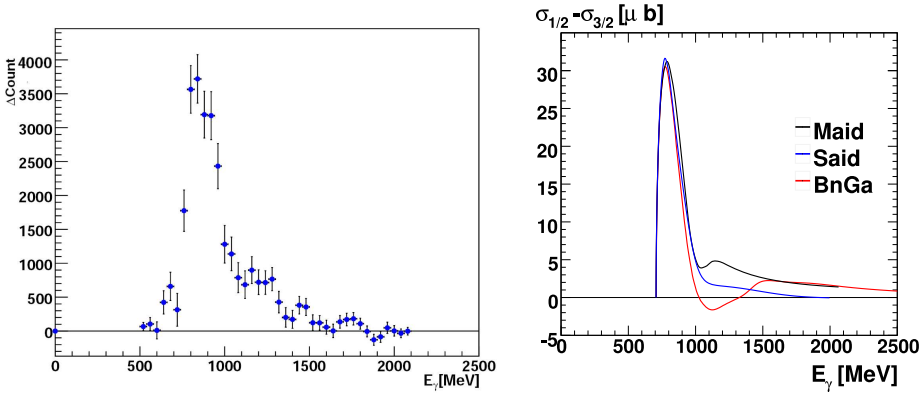


Fig. 8. Left: Raw count rate differences between events with helicity 1/2 and 3/2 ($\Delta = N_{1/2} - N_{3/2}$) in the reaction $\vec{\gamma}\vec{p} \to p\eta$. This data does neither contain corrections for acceptance nor has the polarization and photon flux been taken into account hence its very preliminary status. Right: Predictions for the helicity difference $\sigma_{1/2} - \sigma_{3/2}$ from the BnGa-PWA, MAID and SAID models.

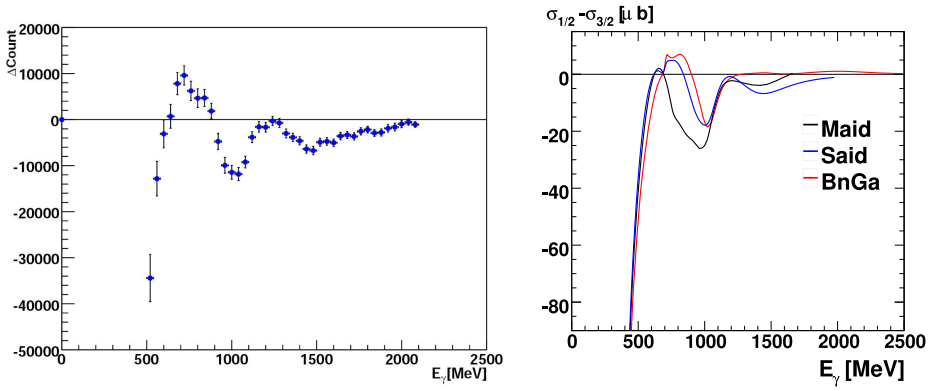


Fig. 9. Left: Raw count rate differences between events with helicity 1/2 and 3/2 ($\Delta = N_{1/2} - N_{3/2}$) in the reaction $\vec{\gamma}\vec{p} \to p\pi^0$. This data does neither contain corrections for acceptance nor has the polarization and photon flux been taken into account hence its very preliminary status. Right: Predictions for the helicity difference $\sigma_{1/2} - \sigma_{3/2}$ from the BnGa-PWA, MAID and SAID models.

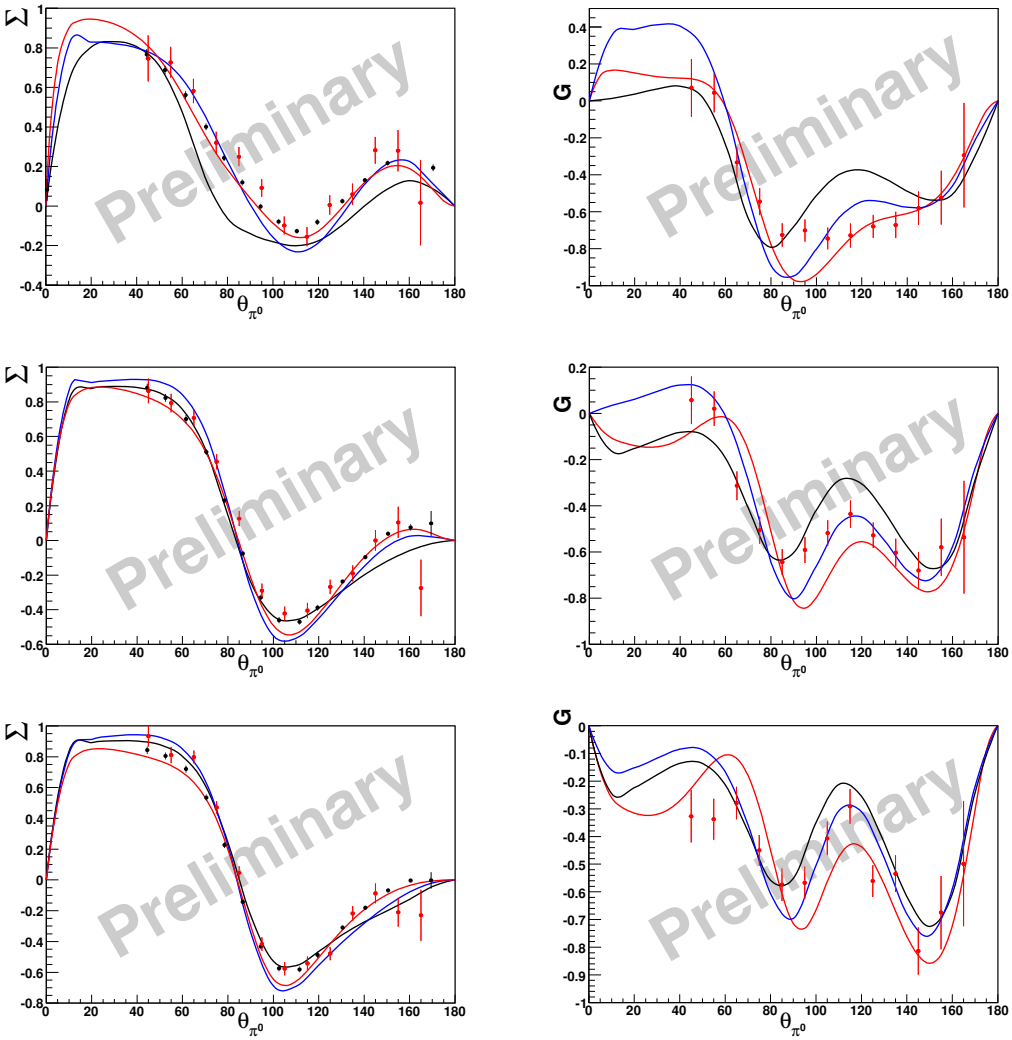


Fig. 10. Left: Preliminary results for $\Sigma$ in $\vec{\gamma}\vec{p} \to p\pi^0$ compared to the GRAAL data and the PWA solutions from BnGa, MAID and SAID. Right: Preliminary results for $G$ in $\vec{\gamma}\vec{p} \to p\pi^0$ compared to the GRAAL data and the PWA solutions from BnGa, MAID and SAID (red, black and blue) for incident photon energies of 966, 1033 and 1066 MeV (top to bottom).

In the second and third resonance region the present raw count rate difference (very preliminary, not corrected for acceptance, polarization and flux not taken into account) indicates positive and negative values, respectively. Fig. 9, right again shows significant differences between the different PWA-models. The sensitivity of $\sigma_{1/2}-\sigma_{3/2}$ on the differences in the PWA, already visible in the total cross section, is of much more pronounced in the differential distributions. Again an almost complete angular coverage will be obtained for the differential distribution. This information is of course very valuable to further constrain the PWAs.

2) Measurements with linearly polarized photons and a longitudinally polarized target.

Using linearly polarized photons the single polarization observable $\Sigma$ and the double polarization observable $G$ can be measured simultanously with a longitudinally polarized target.

The data recently taken at ELSA cover almost the complete solid angle and linear polarization in the energy range of $E_\gamma$=0.4—1.35 GeV.

Figure 10 shows an example of very preliminary results for $\Sigma$ and $G$ taken at the incoming photon energies $E_\gamma$=966, 1033 and 1066 MeV[13]. On the left side the preliminary CBELSA/TAPS results (red points) for $\Sigma$ are compared to the published GRAAL data[14] (black points) and to the solutions of the partial wave analyses BnGa (red), MAID (black) and SAID (blue).

Preliminary results, as e.g. the dilution factor has not been taken into account yet, for the observable $G$ measured for the first time in $\vec{\gamma}\vec{\mathrm{p}} \to \mathrm{p}\pi^0$, are shown on the right side of Fig. 10. Again the experimental results are compared to the predictions from BnGa, Maid and SAID.

The new single and double polarization data obtained with the Crystal-Barrel/TAPS experiment at ELSA will provide new important information for the partial wave analysis. They will resolve the ambiguities in the present solutions and reduce model-dependent uncertainties in the extraction of nucleon resonance parameters, providing a new benchmark for comparisons with QCD-inspired models and lattice calculations.

## References


1 Chiang W, Tabakin F. Phys. Rev. C, 1997, **55**: 2054
2 CBELSA/TAPS publications on single $\pi^0$-photoproduction Bartholomy O et al. Phys. Rev. Lett., 2005, **94**: 012003; van Pee H et al. Eur. Phys. J. A, 2007, **31**: 61
3 CBELSA/TAPS publications on single η-photoproduction Bartholomy O et al., Eur. Phys. J. A, 2007, **33**: 133; Crede V et al. Phys. Rev. Lett., 2005, **94**: 012004; Elsner D et al. Eur. Phys. J. A, 2007, **33**: 147
4 Schmidt A et al. Phys. Rev Lett., 2001, **87**: 232501
5 Beck R et al. Phys. Rev. C, 2000, **61**: 035204
6 Watson K M. Phys. Rev., 1954, **182**: 228
7 Grushin V. Photoproduction of Pions on Nucleons and Nuclei, proceedings of the lebedev Physics Institute Academy of Science of the USSR (Nova Scince Publishers, New York and Budapest, 1989), Vol. 186
8 Ahrens J et al. Phys Rev. Lett., 2002, **88**: 232002
9 Thoma U. Multi-meson-production from CBELSA/TAPS, Proc. NSTAR2009
10 Schmieden H. Vector meson production at ELSA, Proc. NSTAR2009
11 Thoma U, Fuchs M et al. Phys. Lett. B, 2008, **659**: 87
12 Gottschall M. PhD. thesis (in preparation), Bonn (2009)
13 Thiel A. PhD. thesis (in preparation), Bonn (2009)
14 Bartalini O et al. Eur. Phys. J. A, 2005, **26**: 399